ORIGINAL RESEARCH PAPER

Medicine

KEY WORDS: COPD- elastase- Cleome viscosa- iNOS- antioxidants.

POSSIBLE PROTECTIVE EFFECT OF CLEOME VISCOSA IN ELASTASE-INDUCED COPD IN ALBINO RATS

Badr A. Al-Sayed Ph.D., Assistant Professor, Chest Dept., Faculty of Medicine, University of Tabuk

Mohamed E.A. Mostafa Ph.D., Professor, Anatomy Dept., Faculty of Medicine, University of Tabuk & Cairo.

Ashraf M. F. Kamel* Ph.D., Professor, Preparatory Health Sciences Dept., Riyadh Colleges of Dentistry and Pharmacy. *Corresponding Author

ABSTRACT

Background: The possible protective role of Cleome Viscosa (Cl V) administration in experimental chronic obstructive pulmonary disease (COPD) induced by porcine pancreatic elastase (PPE) was investigated.
Material and Methods: Fifty adult male albino rats were divided into four groups; control, sham control, an experimental group that received PPE and a protection group that received Cl V 4 weeks before PPE. Lung specimens were subjected to histological and iNOS immunostaining. Emphysematous changes were quantified by destructive index (DI) and mean linear intercept measurement (Lm).
Results: Administration of Cl V prior to PPE induced marked decrease in the emphysematous areas and in iNOS immune-reaction compared to the experimental COPD group. The DI, Lm and the mean optical density (OD) of iNOS immune-reaction were also significantly reduced with the administration of Cl V.
Conclusion: Cl V administration minimized the histological manifestations of elastase induced COPD.

Introduction:

Chronic obstructive pulmonary disease (COPD) is a term that refers to a large group of lung diseases characterized by the obstruction of air flow that interferes with normal breathing. Emphysema and chronic bronchitis are the most important conditions that compose COPD (Ueno et al., 2015). Emphysema has retained more attention since it is characterized by permanent inflammation and destruction of the alveolar walls, which leads to enlarged air spaces, loss of elastic recoil, reduced gas exchange capacity, and pulmonary hyperinflation (Hind et al., 2009).

COPD is a major cause of morbidity and mortality worldwide. It is the fifth leading cause of death in high-income countries, accounting for 3.8 % of total deaths, and it is the sixth leading cause of death in low- and middle income countries, accounting for 4.9 % of total deaths (Qureshi et al., 2014).

Unfortunately, the COPD prevalence rate in Saudi Arabia is not known because of the lack of population-based epidemiological studies. However, in a study among 501 smokers above 40 years of age attending primary healthcare clinics in three major cities in Saudi Arabia, 71 patients had COPD, accounting for 14.2% of the study population (Al Ghobain et al., 2011). This prevalence rate was similar to the prevalence rate reported in many parts of the world. In another study done in Saudi Arabia to determine the prevalence of respiratory diseases and the length of stay among 810 patients hospitalized with respiratory diseases, COPD was one of the leading causes of hospitalization among patients with respiratory disorders (Alamoudi, 2006).

The main risk factor for the development and progression of COPD is cigarette smoking. Recent data reported alarming and growing evidence that the rate of smoking is steadily increasing among Saudis, that's why we can expect that the COPD prevalence rate in Saudi Arabia is high. Overall, the smoking prevalence in the adult Saudi population is 35% of Saudi males (Al-Khashan et al., 2014). Other documented causes of COPD include occupational dust and chemicals, as well as indoor air pollution from biomass cooking and heating in poorly ventilated dwellings. In contrast to the large amount of experimental research available for other pulmonary inflammatory diseases, experimental models of COPD have not appeared until recently (Wilson et al., 2010).

Elastase-induced COPD is an interesting, low-cost approach, since a single administration may rapidly result in histological and morphological characteristics comparable with those of panacinar emphysema (Antunes and Rocco, 2011). Conversely, prolonged experimental smoke exposure is expensive, slow, and produces centrilobular emphysema (Campbell, 2000).

Cleome viscosa (Cl V) is widely distributed throughout northern and southern Hijaz, Saudi Arabia, especially in Tabuk and is known as Om-Hanif. Traditionally, this plant is used in diarrhea, fever, inflammation, liver diseases, bronchitis, skin diseases, and malarial fever. The juice is useful in piles, lumbago and earache (Jana and Biswas, 2011). The plant contains lignans, flavonoids, saponins, ascorbic acid, and polyunsaturated fatty acid. Its extract has antipyretic, hepatoprotective, anthelminthic, analgesic, anti-inflammatory, antioxidant, immunomodulatory, antimalarial and anti-diarrheal activities (Bose et al., 2011).

To date, only few studies explored the cleome viscosa as a protective agent against COPD.

The aim of the present work is to study the histological changes of the lung of rats after induced COPD. It is also aimed to detect the possible protective effect of CL V when given before onset of COPD by assessing its effects on the degree of inflammation visualized by immunohistochemistry.

Material and Methods:

Drugs and chemicals:

- Porcine pancreatic elastase (PPE) was obtained from Sigma, St. Louis, MO, USA.
- Cleome Viscosa (Cl V) plants were collected from various parts of Tabuk. They were authenticated from the College of Pharmacy, Riyadh Colleges of Dentistry and Pharmacy, Riyadh, Saudi Arabia. The selected parts of the plants were dried in shade at a temperature ranging from 21 to 30°C for 15-30 days. Afterwards, the selected plant parts were chopped and grounded. They were extracted with ethanol in a Soxhlet apparatus. The ethanolic extract was distilled, evaporated, and dried in vacuum. The Cleome viscosa (Cl V) extract was freshly prepared 400 mg/kg doses, dissolved in 1ml ethanol and administered (once daily, orally by gastric gavage) for 4 weeks before elastase administration (Rao et al., 2014).
- All other chemicals were of analytical grade

.

Animals:

This study was carried out on fifty healthy adult male albino rats, aged 20–24 weeks and weighing 185-215 g. The study was conducted at the Animal House of Kasr- Al Aini, Faculty of

Medicine, according to the Ethical Guidelines for the Care and Use of Laboratory Animals. All experimental procedures were conformed to the principles laid down by the National Research Council Guide for the Care and Use of Laboratory Animals with CU-IACUC approval number CUIIIS1516.

Experimental design:
The animals were divided into the following groups:
Group I(normal control group): ten rats received no treatment
.
Group II(sham control group): twenty rats that were subdivided into 2 equal subgroup.
- Subgroup IIa (ethanol-treated group): received 1ml ethanol daily (by gastric gavage) for 7 weeks.
- Subgroup IIb (phosphate –buffered saline treated group): received a single dose of intranasal drop of 100 µl phosphate –buffered saline, four weeks after onset of the experiment.

Group III (COPD-induced group): ten rats. They received a single dose of 50 µL PPE. It was instilled via an intranasal drop, four weeks after onset of the experiment. PPE was dissolved in 100 µl of phosphate-buffered saline (Anciaes et al., 2011).

Group IV(PPE and Cl V- treated group):ten rats. They received daily a single dose of 400 mg/kg Cl V dissolved in 1ml ethanol and administered (by gastric gavage) for 7 weeks, starting 4 weeks before PPE. The animals also received a single dose of 50 µL PPE instilled via an intranasal drop, 4 weeks after Cl V administration.

Induction of COPD:
The animals were anesthetized with an intramuscular injection of ketamine (40 mg/kg) and xylazine (5 mg/kg) before the instillation of porcine pancreatic elastase (PPE). Elastase 50 µl was inhaled via an intranasal drop. It was dissolved in 100 µl of phosphate-buffered saline (Taguchi et al., 2015).

Methods:
Light microscopy:
All animals were sacrificed seven weeks after onset of the experiment by decapitation. Both lungs in each animal were carefully dissected. They were fixed in fresh 2% formaldehyde in 0.1 M phosphate buffer (pH 7.4), dehydrated and embedded in paraffin. Sections of 5µm-thickness were cut, subjected to hematoxylin & eosin staining technique and were examined by light microscope (Bancroft and Gamble, 2002).

Immunohistochemical study:
Lung tissues were fixed in 10% formalin and embedded in parafin. Sections (4 m) were kept overnight at 56 C. Then they were deparafinized with xylene, rehydrated with decreasing percentages of ethanol and finally with water. Antigen retrieval was accomplished by micro-waving slides in citrate buffer (pH 6.0) for 10 min. Slides were left to cool for 20 min at room temperature and then rinsed with distilled water. Surroundings of the sections were marked with a pap pen. The endogenous peroxidase activity was blocked with H2O2 (Lab vision, TA-060-HP, Suffolk, UK) for 10 min at room temperature and later rinsed with distilled water and PBS. Blocking reagent (Lab vision, TA-60-UB) was applied to each slide followed by 5 min incubation at room temperature in a humid chamber. Lung sections were then incubated for 1 h at room temperature with rabbit anti mouse iNOS (iNOS rabbit Pab Neomarker, RB-1605-P) antibodies. Antibodies were diluted in a large volume of UltrAb Diluent (Lab vision, TA-125-UD) at 1:100. The sections were washed in PBS three times for 5 min each time and then incubated for 30 min at room temperature with biotinylated goat anti-rabbit antibodies (Lab vision, TR-060-BN). Slides after being washed in PBS, the streptavidin peroxidase label reagent (Lab vision, TS-060-HR) was applied for 30 min at room temperature in a humid chamber. The colored product was developed by incubation with AEC (Lab vision, TA-004-HAC) for 5 min. The slides were counterstained with hematoxylen and mounted in glycerol gelatin after washing in distilled water (Demirci et al., 2006).

Morphological Analysis:

I. Quantification of emphysema:
Emphysema is a structural disorder characterized by destruction of the alveolar walls and enlargement of the alveolar spaces. We determined destruction of alveolar walls by measuring the destructive index (DI) (Saetta et al., 1985) and enlargement of alveolar spaces by quantifying the mean linear intercept (Lm) (Thurlbeck, 1967; D'hulst et al., 2005; D'hulst et al., 2005), as follows:

A. Morphometry—Parenchymal Destruction
The degree of parenchymal destruction was determined by a microscopic point count technique (Thurlbeck, 1967). This so-called Destructive Index (DI) analysis was performed using a transparent sheet with 50 counting points (Fig. 1). The sheet was laid on an A5-size print, on which the microscopic images from the stained sections were projected using PC_Image 2.1 (Foster Findlay, Newcastle upon Tyne, United Kingdom) and Corel Photopaint 5.0 (Corel Corporation, Ottawa, Canada) software. Images free of large bronchi(oli), vessel, collapsed tissue, or extensive fibrosis were selected. The final magnification of the images was x100. From each lung specimen, an average of 5 different sections was used, and in the sections generally 3 to 10 representative nonoverlapping fields were selected, depending on the histomorphology of that section. Alveolar and duct spaces lying underneath the counting points were evaluated for the presence of destruction. Destruction was defined on base of one or more of the following criteria: (a) at least two alveolar wall defects, (b) at least two intraluminal parenchymal rags in alveolar ducts, (c) clearly abnormal morphology, or (d) classic emphysematous changes (Thurlbeck, 1967). Microscopic fields in which more than 20% of the points coincided with vessels, or conducting airways were excluded because they might be confused with enlarged alveolar spaces. Fields with alveolar and ductular spaces with a minimum diameter of more than 0.6 mm were also excluded. The percentage of all the points falling into the several categories of destroyed air spaces was computed to reveal the Destructive Index, using the formula [D/(D+N)] x100%, where D = destroyed, and N = normal.

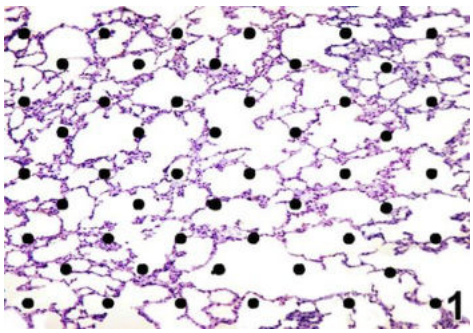

Fig. 1: Schematic representation of the Destructive Index analysis. A transparent sheet with 50 equally distributed points is laid over the printed digitized image of a HE-stained section. For each dot the area surrounding that dot is determined according the criteria mentioned in the Methods section.

B. Morphometry—Air Space Enlargement
Enlargement of air spaces was evaluated in the Mean Linear Intercept (Lm) measurement technique, originally described by Dunnill (1962). The Mean Linear Intercept represents the average size of alveoli. The same printed images as described above were used. To measure the intercepts, a transparent sheet with 10 horizontal and 11 vertical lines was laid over the images (Fig. 2). The intercepts of alveolar walls with these lines were counted. Intercepts of bronchioli, blood vessels or septa were counted for one half since they are more or less part of the structure of surrounding alveolar spaces (Dunnill, 1962). Images with bronchi, large bronchioli or blood vessels were excluded from the measurements because they might be confused with enlarged alveolar spaces. Images showing compression of alveolar space - observed as meandering walls - were also excluded. Values were corrected for tissue shrinkage which occurs with histological processing. The correction factor was 0.82, in accordance with

data from Weibel (1963). As with the Destructive Index, a minimum of 3 non-overlapping fields per specimen were analyzed.

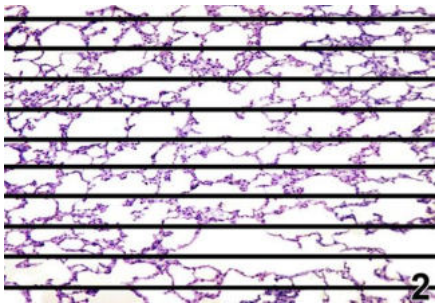

Fig. 2: Schematic representation of the Mean Linear Intercept analysis. A transparent sheet with 10 equally distributed horizontal lines is laid over the printed digitized image of a HE-stained section. A transparent sheet with 11 equally distributed vertical lines is used thereafter (not shown). For each line the intercepts with the tissue structures is counted according the criteria mentioned in the Methods section.

II. Morphometric Quantification of iNOS immunoreactivity:

Optical density (OD) of iNOS:

The optical density of iNOS reactions were measured in ten lung fields per specimen at a magnification of 100. The measurements were obtained by using Leica Qwin 500 image analyzer computer system, England (Mroz et al, 2015).

Statistical analysis:

Quantitative data (Mean Linear Intercept, Destructive Index, and optical density of iNOS reactions) were expressed as the mean and standard deviation (±SD). Differences between the groups were analyzed using an analysis of variance (ANOVA). When the significant differences were detected, the ANOVA was followed by an unpaired two-tailed Student's t-test. Correlation coefficients were calculated using Pearson's rank correlation test. A value < 0.05 was considered statistically significant. All statistical analyses were performed by using SPSS statistical software for Windows version 22, SPSS Inc., Chicago, IL., USA (Mould, 1989).

Results:

Light microscopic results:

Sections in the lungs of rats from **group I** (control group) revealed preserved pulmonary architecture, alveolar ducts, alveolar sacs and alveoli. The alveoli were surrounded and separated from each other by thin interalveolar septa (Figs. 3a & 3b). They were lined by two types of pneumocytes; type I pneumocytes which were flat cells with flat nuclei and type II pneumocytes which appeared as cuboidal or rounded cells with rounded nuclei (Fig. 3c). The interalveolar septa were formed of the epithelial lining of the alveoli and a loose connective tissue (Fig. 3c). Small branches of bronchial arterioles were seen accompanying the bronchioles while small branches of pulmonary arterioles were seen among the alveoli (Fig. 3a). The bronchioles appeared surrounded by thin layer of smooth muscle layer and devoid of cartilage plates. The bronchioles were lined by folded simple columnar ciliated epithelium and Clara cell (Fig. 3d).

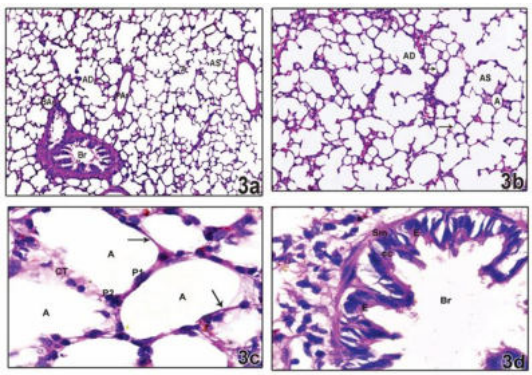

Fig.3: Photomicrographs of sections in the lungs of the control rat (group I) stained with H & E showing preserved pulmonary architecture. **Fig.3a** presents preserved alveolar ducts (AD), alveolar sacs (AS) and alveoli (A) are observed. The alveoli are surrounded and separated from each other by thin interalveolar septa (arrows). Thin walled pulmonary arterioles (PAr) are seen among the alveoli. A bronchiole (Br) is seen accompanied by thin walled bronchial (BAr) arteriole **(X100).Fig.3b** shows preserved alveolar ducts (AD), alveolar sacs (AS) and alveoli (A) are observed. The alveoli are surrounded and separated from each other by thin interalveolar (arrows) septa **(X200).Fig.3c** presents alveoli (A) lined by alveolar epithelium composed of two types of cells; type I pneumocytes (P1) which are flat cells with flat nuclei and type II pneumocytes (P2) which are cuboidal or rounded cells with rounded nuclei. The alveoli are separated from each other by thin interalveolar septa (arrows) which are formed of the alveolar epithelial lining and loose connective (CT) tissue **(X1000).Fig.3d** shows the bronchioles (Br) surrounded by thin layer of smooth muscle layer (Sm) and devoid of cartilage plates. The bronchiole is lined by folded simple columnar ciliated epithelium (E) and Clara (cc) cell. **(X1000)**

Sections of the lungs of rats from **groups IIa & IIb** showed no obvious changes from group I.

In PPE- treated group III, the lungs showed emphysematous areas (Figs.4a, c, d & e) with loss of alveolar walls, enlargement of alveolar spaces and decreased alveolar wall attachment. The alveoli are collapsed with thickened septa (Fig. 4b). The pulmonary (Fig. 4a) and bronchial arteries (Fig. 4d) are thickened. Some sections presented cellular infiltration around the bronchiole including neutrophils**,** eosinophil and macrophages which contain hemosiderin Lydig granules. Few type II pneumocytes and apoptotic like cells were seen (Fig. 4f).

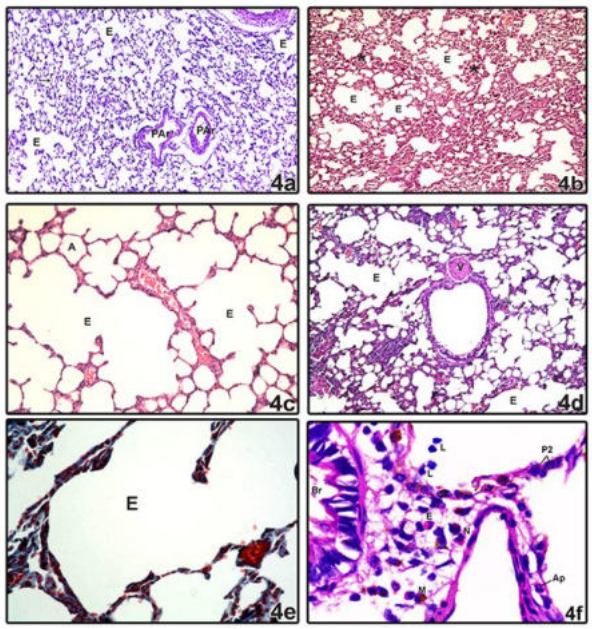

Fig. 4: Photomicrographs of sections in the lungs of the rats of the experimental group (group III) stained with H & E showing emphysematous (E) areas **(4a, 4c, 4d & 4e).** The alveoli are collapsed with thickened septa **(4b)**. The pulmonary (P Ar) arteries **(4a)** and bronchial (Br A) vessels **(4d)** are thickened **(4a, 4b X100, 4c, 4d X200 & 7e X 400). Fig.4f:** presents showing cellular infiltration around the bronchiole **(Br)** including neutrophils **(N),** eosinophil **(E)** and macrophages **(M)** contain hemosedrin Lydeg granules. Few type II pneumocytes **(P2)** are seen. Apoptotic like cells **(Ap)** can be observed. **(X1000).**

Administration of Cl V previous to PPE in **Group IV** presented marked decrease in the emphysematous areas within relatively normal areas compared to group III. The inter-alveolar septa are thickened (Figs. 5a-c). Areas of chronic inflammation (Fig. 5b),

blood within congested capillaries (Fig. 5c) can be seen. The bronchioles had thickened smooth muscles. Alveoli were lined by alveolar epithelium composed of two types of cells; type I pneumocytes and type II pneumocytes which were cuboidal or rounded cells with rounded nuclei (Fig. 5d).

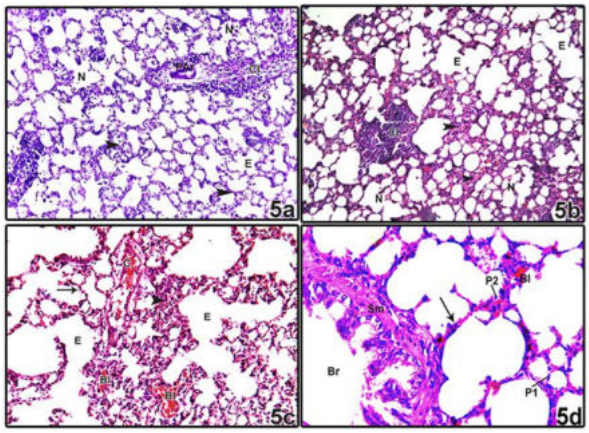

Fig.5: Photomicrographs of sections in the lungs of the rats of the CL V protected group (group IV) stained with H & E showing decreased emphysematous areas (E) within relatively normal area (N). The inter-alveolar septa are thin (arrow) in certain areas and thickened (arrow heads) in other areas. Areas of chronic inflammation (CI), blood (Bl) within congested capillaries (C) can be seen. The bronchioles (Br) have thickened smooth muscles (Sm). Alveoli are lined by alveolar epithelium composed of two types of cells; type I pneumocytes (P1) and type II pneumocytes (P2) which are cuboidal or rounded cells with rounded nuclei. **(5a, 5b X100, 5c X200 & 5d X400).**

Immunohistochemical results:

Immunostaining with iNOS was of normal distribution in section of rats belonging to control (I) group and vehicle (II) group (Fig. 6a). It is maximally increased distribution in PPE- treated group III (Fig. 6b). It is markedly decreased but still more than normal in group IV (Fig. 6c).

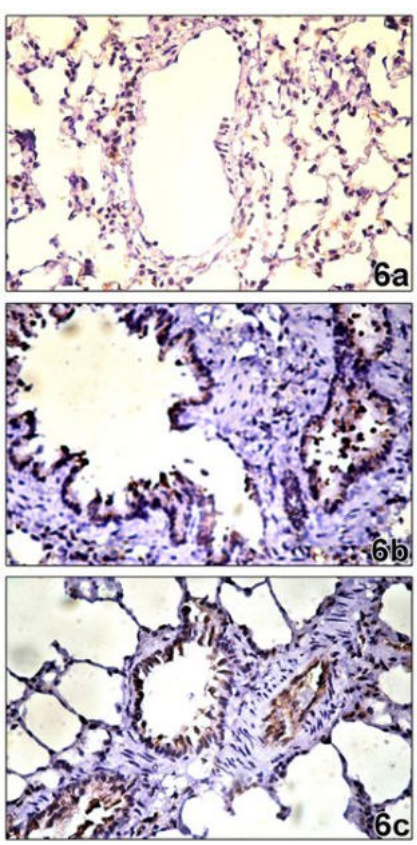

Fig.6: Photomicrographs of protection lung sections immunostained with iNOS showing 6a: Control lung with normal distribution of iNOS, 6b: Experimental lung showing increased iNOS and 6c: decreased iNOS immunostained areas. **(6a, 6b & 6cX200).**

Morphometric Results:

I. Morphometric qualification of emphysema

Destructive index (DI) and Mean Linear Intercept (Lm):

The results of the morphometric investigation of the lungs are given in table (1) and (Figs. 7-9). The destruction of the alveolar walls was quantified by measuring the destructive index (DI) while the enlargement of the alveolar spaces was quantified by measuring the mean linear intercept (Lm).

It was found that DI and Lm were significantly higher in experimental COPD rats than in control rats, while Lm was significantly increased (P<0.05) in experimental COPD rats. Administration of Cleome viscosa significantly reduced (P<0.05) both DI and Lm compared to those of experimental COPD rats.

Table (1): Comparing the DI, Lm, and OD of iNOS for all groups

	Control	Group III	Group IV
Mean (± SD) of DI (%)	52.9 ± 13.62	69.2 ± 15.37•	59.8 ± 11.99*
Mean (± SD) of L_m (µm)	324 ± 64	376 ± 71•	328 ± 57*
Mean (± SD) OD of iNOS (%)	0.224 ± 0.0386	0.393 ± 0.0266•	0.309 ± 0.0324*

•Significant compared to control group (P<0.05)
*Significant compared to experimental COPD group (P<0.05)

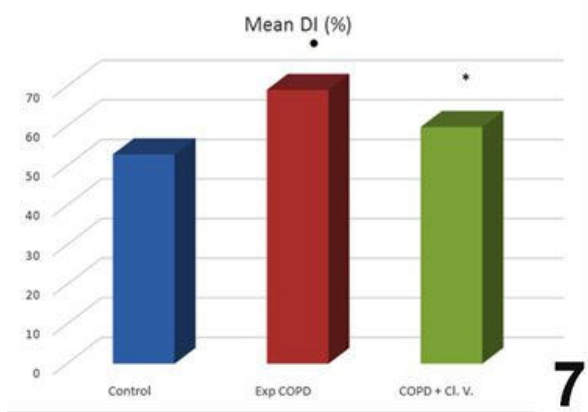

Fig.7: A histogram showing mean destructive index (DI) among the different groups. Mean DI is significantly ( ) higher (P<0.05) in experimental COPD rats than in control rats. Administration of Cl V significantly (*) reduced (P<0.05) DI compared to those of experimental COPD rats.

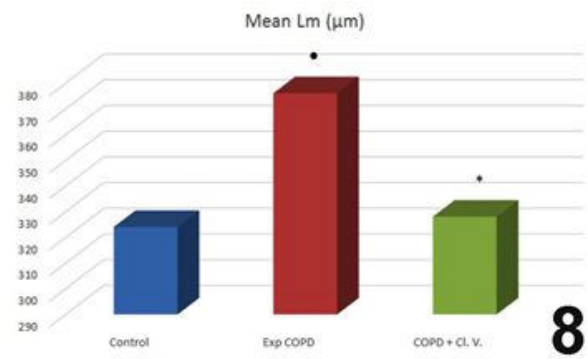

Fig.8: A histogram showing Mean Linear Intercept (Lm) among the different groups. Mean Lm is significantly ( ) higher (P<0.05) in experimental COPD rats than in control rats. Administration of Cl V significantly (*) reduced (P<0.05) Lm compared to those of experimental COPD rats.

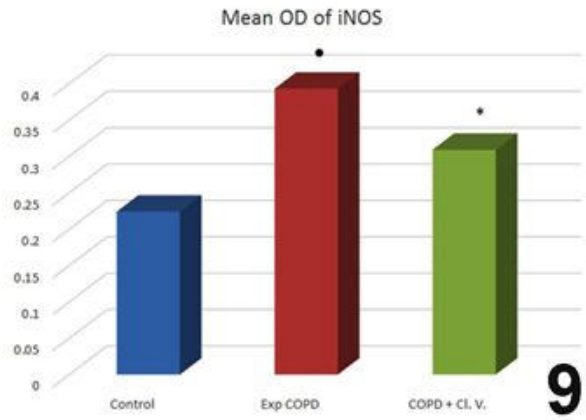

Fig.9: A histogram showing Optical Density (OD) of iNOS among the different groups OD is significantly ( ) higher (P<0.05) in experimental COPD rats than in control rats. Administration of Cl V significantly (*) reduced (P<0.05) OD compared to those of experimental COPD rats.

II. Morphometric qualification of iNOS immunoreactivity:

Optical density of iNOS immune-reaction:

Using the image analysis computer system, it was found that experimental COPD (group III) significantly increased (P<0.05) the mean optical density of iNOS immune-reaction in relation to the control. Moreover, when compared to the experimental COPD group (group III), the mean optical density of iNOS immune-reaction significantly decreased (P<0.05) by administration of Cl V (Table 1 & Fig. 9).

Discussion:

Chronic obstructive pulmonary disease (COPD) is a major incurable global health burden. The morbidity and mortality of COPD continue to increase and will become the third largest cause of death in the world by 2020 (Vestbo et al., 2013).

The aim of this study was to evaluate the protective possible effect of Cl V on COPD by assessing its effects on the degree of inflammation visualized by immunohistochemistry.

Over years, prolonged smoke exposure was used to induce experimental COPD. But the chronic use of cigarette smoke in induction of COPD is expensive, slow, and produces centrilobular emphysema (Antunes and Rocco, 2011). Moreover, the degree of COPD induced by cigarette smoking can be influenced by smoke concentration animal strains and sex (Vecchio et al., 2013). On the other hand, porcine pancreatic elastase (PPE) offers the advantages of being inexpensive, since single administration may rapidly result in histological and morphological characteristics compatible with those of panacinar emphysema (Oliveira et al., 2016). Moreover, it causes more widespread lung damage (Antunes and Rocco, 2011).

In the present work, In PPE- treated group III, the lungs showed areas of the lungs with loss of alveolar walls, enlargement of alveolar spaces. These results were with agreement with those of Zheng et al. who described areas of lung parenchyma with enlargement of air spaces. They added that some alveoli were merged (Zheng et al., 2009).

The existing study presented some sections with cellular infiltration around the bronchioles. The cells included neutrophils, eosinophil and macrophages which contained hemosiderin Lydig granules. This coincides with the results previously reported by Zheng et al. who observed increase in number of neutrophils and macrophages in COPD (Zheng et al., 2009). Moreover, Algaem et al. (2103) reported accumulation of inflammatory cells that occluded the bronchioles and the alveolar sac, with thickness of alveolar smooth muscle and trachea. Furthermore, Lin et al. found increased number of the infiltrated inflammatory cells in the COPD model animals (Lin et al., 2016).

The role of macrophages in COPD was elucidated by Retamales et al. who proposed that macrophages become activated and release proinflammatory cytokines, such as tumor necrosis factor- alpha, interleukin which amplify lung inflammation and contribute to disease progression (Retamales et al., 2001). Moreover, they added that macrophages also release several chemokines that attract circulating cells into the lungs, which later differentiate into macrophages within lung tissue. Moreover, Antunes and Rocco (2011) posted that macrophages and neutrophils contribute to persistent inflammation and to an oxidant/antioxidant imbalance by releasing reactive oxygen species (ROS) that induce epithelial and endothelial cell apoptosis and inactivate antiproteolytic defense mechanisms, such as tissue inhibitors of metalloproteases and alpha-1 antitrypsin.

Lung sections in COPD-induced rats in the present work showed collapsed alveoli with thickened septa. The pulmonary and bronchial arteries were thickened. These finding are in line with those reported by Jeffery who reported an increased inflammatory infiltrate with thickened septa between alveoli. He found also an increase in thickness of bronchial arteries in COPD (Jeffery, 1992).

In the current study, there were few type II pneumocytes and apoptotic like cells. Type II cells were described by Serrano-Mollar et al. (2007), that synthesize, store, and secrete pulmonary surfactant, which reduces alveolar surface tension and stabilizes alveolar units for efficient gas exchange. Moreover, Zhao et al. (2010), added that type II pneumocytes secrete a variety of cytokines and proteins that can modify the inflammatory response and oxidative stress response and inhibit fibroblast proliferation and collagen synthesis which are implicated in the pathogenesis of COPD. Furthermore, Hou et al. (2013), mentioned that apoptosis of lung epithelial cells is one of the potential factors involved in the pathogenesis of COPD.

Administration of Cl V previous to PPE in the present study presented marked decrease in the emphysematous areas within relatively normal areas compared to group III. The inter-alveolar septa are thickened. Areas of chronic inflammation, blood within congested capillaries can be seen. The bronchioles had thickened smooth muscles. Alveoli were lined by alveolar epithelium composed of two types of cells; type I pneumocytes and type II pneumocytes which were cuboidal or rounded cells with rounded nuclei. The protective effect of Cl V may be attributed to its antioxidant effect (Jayaprakash et al., 2016). They studied the anti-oxidant, cytotoxic and anticancer properties of Cl V extract. They screened carbohydrates, glycosides, flavonoids, phytosterols and triterpenoids in the plant. Pillai and Nair evaluated the reactive oxygen species (ROS) scavenging and in vitro antioxidant activities of Cleome, C. viscosa. They used different assays such as FRAP, DPPH, ABTS, hydroxyl, superoxide, nitric oxide, and hydrogen peroxide. The extracts gave positive results for all the assays (Pillai and Nair, 2013).

Immunostaining with iNOS of the existing work was of normal distribution in section of rats belonging to control (I) group and vehicle (II) group. It was maximally increased distribution in PPE-treated group III. It was markedly decreased but still more than normal in group IV. These results are in line with those of Demirci et al. who reported that minimal iNOS reactivity in control group and maximal increase was detected in infected mice in lungs and liver (Demirci et al., 2006). Moreover, Seimetz et al. found mice lacking iNOS were protected against emphysema (Seimetz et al., 2011). Furthermore, Malerba et al. (2014) explained the increase in iNOS expression in COPD due to increase in endogenous mediators as chemokines and cytokines.

In the current study, It was found that DI and Lm were significantly higher in experimental COPD rats (DI 69.2 ± 15.37% & Lm 376 ± 71 µm) than in control rats (DI 52.9± 13.62% & Lm 324 ± 64 µm), while Lm was significantly increased (P<0.05) in experimental COPD rats. Administration of Cleome viscosa significantly reduced (P<0.05) both DI and Lm (DI 59.8 ± 11.99% & Lm 328 ± 57 µm) compared to those of experimental COPD rats. Less results were obtained by Saetta et al. (1985) who found significant differences (P<0.005) between DI and Lm of smokers (DI 47.1 ± 15.1% & Lm

343 ± 77 µm) and nonsmokers (DI 16.8 ± 6.5% & Lm 297 ± 46 µm). On the other hand, more destructive index (45%) was reported by Reyna-Sepúlveda et al. in experimental animals and 44% in control group (Reyna-Sepúlveda et al., 2016).

Mean optical density (OD) of iNOS immune-reaction was studied in the current study using the image analysis computer system. It revealed that there was significant increase (P<0.05) of OD of the experimental group (0.393% ± 0.0266) in relation to the control (0.224% ± 0.0386). Moreover, when compared to the experimental COPD group, the OD significantly decreased (P<0.05) by pre-administration of Cleome viscosa (0.309% ± 0.0324). These results were in line with those obtained by Mroz et al. who tested the anti-inflammatory of atorvastatin in COPD patients. They found significant decrease (P<0.05) of the mean OD of lung biopsies of COPD patients [62.51%] compared to those after atorvastatin treatment [27.01%] (Mroz et al., 2105).

In conclusion, Cl V preserved the normal histological architecture of the lung and minimized the manifestations of COPD induced experimentally by administration of elastase. This beneficial effect of Cl V was mostly related to its antioxidant and anti-inflammatory properties. Cleome Viscosa proved to be both effective and safe. The results of the present investigation may trigger an interest in using Cl V to prevent COPD in high risk individuals.

Acknowledgement:
The authors would like to express their sincere gratitude to the deanship of scientific research, University of Tabuk, for generously funding this work.

References:

1. Al Ghobain M, Al-Hajjaj M S, Wali S O. Prevalence of chronic obstructive pulmonary disease among smokers attending primary healthcare clinics in Saudi Arabia. Ann Saudi Med., 2011; 31:129–33. doi: 10.4103/0256-4947.77485.
2. Aamoudi O S. Prevalence of respiratory diseases in hospitalized patients in Saudi Arabia: A 5 years study 1996-2000. Ann Thorac Med., 2006; 1:76–80. DOI: 10.4103/1817-1737.27106.
3. Algaem MA, Numan IT, Hussain SA. Effects of valsartan and telmisartan on the lung tissue histology in sensitized rats. Am J Pharmacol Sciences, 2013; 1, (4): 56-60. DOI: 10.12691/ajps-1-4-3.
4. Al-Khashan HI, Al Sabaan FS, Al Nasser HS, et al. The prevalence of smoking and its associated factors among military personnel in Kingdom of Saudi Arabia: A national study. J Family Community Med., 2014; 21(3): 147-153. doi: 10.4103/2230-8229.142966.
5. Anciaes AM, Olivo CR, Prado CM, et al. Respiratory mechanics do not always mirror pulmonary histological changes in emphysema. Clinics (Sao Paulo), 2011; 66(10):1797–1803. doi: 10.1590/S1807-59322011001000020.
6. Antunes MA, Rocco PR. Elastase-induced pulmonary emphysema: insights from experimental models. An Acad Bras Cienc., 2011; 83 (4): 1385-1395. PMID:22159348.
7. Bancroft JD, Gamble M. (2002): Theory and practice of histological techniques. 5th ed, Churchill-Livingstone, London, Edinburgh, New York, Philadelphia, St Louis, Sydney and Toronto, 377-694.
8. Bose U, Bala V, Ghosh TN, at al. Rev. bras. farmacogn. Braz J of Pharmacognosy., 2011; 21(1): 165-169. doi: 10.1590/S0102-695X2011005000023.
9. Campbell EJ. Animal models of emphysema: the next generations. J Clin Invest., 2000; 106(12): 1445–1446. PMCID: PMC381478, doi: 10.1172/JCI11791.
10. D'hulst AI, Maes T, Bracke KR, et al. Cigarette smoke-induced pulmonary emphysema in scid-mice. Is the acquired immune system required? Respir Res., 2005; 6: 147-156. PMID: 16359546, PMCID: PMC1334210, doi: 10.1186/1465-9921-6-147.
11. D'hulst AI, Vermaelen KY, Brusselle GG, et al. Time course of cigarette smoke-induced pulmonary inflammation in mice. Eur Respir J., 2005; 26: 204–213. PMID: 16055867, doi: 10.1183/09031936.05.00095204.
12. Demirci C, Gargili A, Kandil A, et al. Inhibition of inducible nitric oxide synthase in murine visceral larva migrans: effects on lung and liver damage. Chin J Physiol., 2006; 49(6): 326-334. PMID:17357539.
13. Dunnill MS. Quantitative methods in the study of pulmonary pathology. Thorax, 1962; 17 (4):320–328. PMCID: PMC1018718.
14. ind M, Stinchcombe S, Palovarotene, A novel retinoic acid receptor gamma agonist for the treatment of emphysema. Curr Opin Investig Drugs., 2009; 10: 1243–1250. PMID:19876792.
15. Hou HH, Cheng SL, Liu HT, et al. Elastase induced lung epithelial cell apoptosis and emphysema through placenta growth factor. Cell Death and Dis., 2013; 4, e793; doi:10.1038/cddis.2013.329.
16. Jana A, Biswas SM. Lactam nonanic acid, a new substance from Cleome viscosa with allelopathic and antimicrobial properties. Journal of Biosciences, 2011; 36(1): 27-35. doi: 10.1007/s12038-011-9001-9.
17. Jayaprakash AP, Krishnakumar KR, Srinivasan KK, et al. Evaluation of antioxidant, cytotoxic and anticancer effects of Cleome Viscosa Linn. European journal of pharmaceutical and medical research, 2016; 3(4): 253-262.
18. Jeffery PK. Histological features of the airways in asthma and COPD Respiration, 1992; 59 Suppl 1:13-16. PMID: 1579725
19. Lin J, Xu F, Wang G, et al. Paeoniflorin attenuated oxidative stress in rat COPD model induced by cigarette smoke. Evidence-Based Complementary and Alternative Medicine, 2016; Article ID 1698379, http://dx.doi.org/10.1155/2016/1698379
20. Malerba M, Radaeli A, Olivini A, et al. Exhaled nitric oxide as a biomarker in COPD and related comorbidities. Biomed Rese Int., 2014; 2014, Article ID 271918, PMID: 24719850, PMCID: PMC3955647, doi: 10.1155/2014/271918
21. Mould RF. Introductory Medical Statistics. 2nd ed., Adam Hilger, Bristol, Philadelphia, 1989;17, 22 & 26.
22. Mroz RM, Lisowski P, Tycinska A, et al. Anti-inflammatory effects of atorvastatin treatment in chronic obstructive pulmonary disease. A controlled pilot study. J of physiol pharmacol., 2015; 66 (1): 111-128. PMID: 25716971.
23. Oliveira MVde, Silva PL, Rocco, PRM. Animal models of chronic obstructive pulmonary disease exacerbations: A Review of the Current Status. J Biomed sciences, 2016; 5: 1-8, doi: 10.4172/2254-609X.100022.
24. Pillai LS, Nair BR. Radical scavenging potential of cleome viscosa L. and cleome burmanni W. & A. (cleomaceae). International journal of pharmaceutical sciences and research, 2013; 4 (2): 698-705.
25. Qureshi H, Sharafkhaneh A, Hanania N A. Chronic obstructive pulmonary disease exacerbations: latest evidence and clinical implications. Ther. Adv. Chronic Dis., 2014; 5(5):212-227. doi: 10.1177/2040622314532862.
26. Rao BS, Reddy KE, Parveen K, et al. Effects of Cleome viscosa on hyperalgesia, oxidative stress and lipid profile in STZ induced diabetic neuropathy in Wistar rats. Pak J Pharm Sci., 2014; 27(5), 1137-1145. PMID: 25176371.
27. Retamales I, Elliott WM, Meshi B, et al. Amplification of inflammation in emphysema and its association with latent adenoviral infection. Am J Respir Crit Care Med., 2001; 164: 469-473. PMID: 11500352, doi: 10.1164/ajrccm.164.3.2007149
28. Reyna-Sepúlveda F, Caballero-Mendoza E, Guzmán-de-la-Garza F, et al. Emphysema model in rats exposed to tobacco smoke. Morphometric and functional analysis. Medicina Universitaria, 2016; 18(71):79-84. http://dx.doi.org/10.1016/j.rmu.2016.05.004.
29. Saetta M, Shiner RJ, Angus GE, Kim WD, Wang NS, King M, Ghezzo H and Cosio MG. Destructive index: a measurement of lung parenchymal destruction in smokers. Am Rev Respir Dis., 1985; 131: 764–769. PMID: 4003921, doi: 10.1164/arrd.1985.131.5.764.
30. Seimetz M, Parajuli N, Pichl A, et al. Inducible NOS inhibition reverses tobacco-smoke-induced emphysema and pulmonary hypertension in mice. Cell, 2011; 147 (2): 293–305. PMID: 22000010, doi: 10.1016/j.cell.2011.08.035.
31. Serrano-Mollar A, Nacher M, Gay-Jordi G, et al. Intratracheal transplantation of alveolar type II cells reverses bleomycininduced lung fibrosis. Am J Resp Crit Care, 2007;
176(12): 1261-1268. PubMed: 17641155, DOI:
http://dx.doi.org/10.1164/rccm.200610-1491OC.
32. Taguchi L, Pinheiro NM, Olivo CR, et al. A flavanone from Baccharis retuca (Asteraceae) prevents elastase-induced emphysema in mice by regulating NF-kB, oxidase stress and metalloproteinases. Respir Res., 2015; 16:79. doi: 10.1186/s12931-015-0233-3.
33. Thurlbeck WM. Measurement of pulmonary emphysema. Am Rev Respir Dis., 1967; 95(5): 752–764. PMID: 5337140.
34. Ueno M, Maeno T, Nishimura S, Ogata F, et al. Alendronate inhalation ameliorates elastase induced pulmonary emphysema in mice by induction of apoptosis of alveolar macrophages. Nat commun., 2015; 6 (6332): 1-13. doi:10.1038/ncomms7332.
35. Vecchio D, Arezzini B, Pecorelli A, et al. Reactivity of mouse alveolar macrophages to cigarette smoke is strain dependent. Am J Physiol Lung Cell Mol Physiol., 2010; 298: L704-L713. PMID: 20154225, doi: 10.1152/ajplung.00013.2009.
36. Vestbo J, Hurd SS, Agusti AG, et al. Global Strategy for the diagnosis, management and prevention of chronic obstructive pulmonary disease: GOLD Executive Summary. Am J Respir Crit Care Med., 2013; 187: 347–365. PMID: 22878278, doi: 10.1164/rccm.201204-0596PP.
37. Weibel ER. Principles and methods for the morphometric study of the lung and other organs. Lab Invest., 1963; 12:131–155, PMID:13999512.
38. Wilson AA, Murphy GJ, Hamakawa H, et al. Amelioration of emphysema in mice through lentiviral transduction of long-lived pulmonary alveolar macrophages. J Clin Invest., 2010; 120(1): 379–389. doi: 10.1172/JCI36666.
39. Zhao C, Fang X, Wang D, et al. Involvement of type II pneumocytes in the pathogenesis of chronic obstructive pulmonary disease. Resp Med., 2010; 104: 1391-1395. http://dx.doi.org/10.1016/j.rmed.2010.06.018
40. Zheng H, Liu Y, Huanga T, et al. Development and characterization of a rat model of chronic obstructive pulmonary disease (COPD) induced by side stream cigarette smoke. Toxicol Lett., 2009; 189: 225–234. PMID: 19524650, doi: 10.1016/j.toxlet.2009.06.850.